

Synthesis and characterization of hybrid composite aerogels from alginic acid and graphene oxide

C J U Co^{1,2}, A T Quitain², J Q Borja¹, N P Dugos¹, M Takafuji², T Kida²

¹Department of Chemical Engineering, De La Salle University, Malate, Manila, Philippines 1004

²Department of Applied Chemistry and Biochemistry, Kumamoto University, Kumamoto, Japan 860-0862

*E-mail: clarence_co@dlsu.edu.ph

Abstract. Aerogels are one class of solid adsorbents that are gaining considerable attention because of their very high porosity, high specific surface area, and extremely low density. However, most aerogels being studied and used recently are synthetic in nature, which are usually mesoporous silica and metal-organic frameworks (MOFs). As research focus is geared towards sustainable engineering, it is desired to utilize biomass to synthesize aerogels. This study thus aims to produce alginic acid-graphene oxide hybrid composite aerogels and compare them with its existing synthetic counterparts. Alginic acid (AA) is an abundant marine biopolymer that easily forms gels, while graphene oxide (GO) is a nanomaterial consisting of many functional groups. Aerogels made up of AA and GO were successfully synthesized using a sol-gel method. The hydrogel was converted into an aerogel by drying with supercritical carbon dioxide. The percentage of graphene oxide was varied from 0 to 20%. The aerogels were characterized by scanning electron microscopy (SEM), Fourier Transform Infrared Spectroscopy (FTIR), X-ray diffraction (XRD), thermogravimetric analysis (TGA) and nitrogen adsorption-desorption measurements. The addition of GO increased the specific surface area of the aerogel up to a certain point, after which it decreased. The 10% GO-AA aerogel showed the most favourable porosity characteristics with a specific surface area of 177.26 m²/g and average pore diameter of 53.2 nm. There had been no observable difference in the thermal behaviour of the aerogels with a change in the concentration of graphene oxide.

1. Introduction

Solid adsorbents are being used nowadays in numerous applications: adsorption of metal ions from solution [1], adsorption of dyes [2][3], selective adsorption of gases from bulk gas [4][5], and even as drug carrier systems [6][7], among several others. They are also being eyed as a potential instrument in wastewater treatment [8].

There are several kinds of solid adsorbents being studied in literature, the prominent ones being mesoporous silica, metal-organic frameworks (MOFs), and activated carbon [9]. Yet another class of adsorbents, aerogels, are gaining attention because of their high specific surface area, porosities near unity and very well connected pore space. Aerogels are hydrogels which the liquid content (usually water) contained in the solid framework of the gel is replaced with a gas, leaving behind a porous structure. This cannot be accomplished through air or ambient drying, as passing through the liquid-gas interface would cause capillary pressure to collapse the structure. In order to avoid it, the liquid-gas interface is circumvented by using either freeze drying or supercritical drying [10].

Hybrid composites are materials which have two or more components mixed in the nanoscale level. Although at that level, the mixture seems heterogeneous, at the macroscopic level, they have uniform properties. In addition, formations of hybrid composites have sometimes found to produce a



synergistic effect, that is, the characteristics of the composite turns out to be better than either starting species [11]. Thus, it is of great interest that this principle be applied in the current study.

In the selection of the materials to be used for the hybrid composite aerogel, it was deemed by the authors that the current trend today is towards biomass utilization, as greener and environmentally-safe industrial products are pursued, and nanoscale technology, which has brought about new materials with unique properties and applications.

As such, in this study, hybrid composite aerogels were formed from the combination of a bio-based polymer, alginic acid, and graphene oxide. Alginic acid is cheap, abundant and can be easily gelled. On the other hand, graphene oxide is a flat molecule with numerous oxygen-containing functionalities, which has a high surface area and acts as a nanofiller [12]. The aerogels formed from this study is promising as it can be used as an adsorbent for different applications.

2. Experimental Procedure

2.1. Reagents and Chemicals

For the synthesis of graphene oxide, powdered graphite, sodium nitrate, potassium permanganate, concentrated sulfuric acid, hydrogen peroxide (30%) and concentrated hydrochloric acid were purchased from Wako Pure Chemical Industries, Ltd. All were used as supplied except for the concentrated hydrochloric acid, which was diluted to 5%.

For the synthesis of the hybrid composite aerogel, alginic acid and sodium hexametaphosphate were purchased from Wako Pure Chemical Industries, Ltd. Calcium hydrogenphosphate dihydrate was purchased from Nacalai Tesque, Inc. and D-(+)-glucono-1,5-lactone (GDL) from Tokyo Chemical Industry Co.

2.2. Methods

2.2.1. Synthesis of Graphene Oxide. The first step was the synthesis of graphene oxide (GO) which was done using a modified Hummer's Method as reported by Koinuma et al. [13]. To produce one batch of GO, four grams of graphite powder and four grams of sodium nitrate were dissolved in 184 mL of concentrated sulfuric acid in a 2-L beaker under an ice bath with vigorous stirring using a magnetic stirrer for 30 minutes. Twenty grams of potassium permanganate was slowly added into the solution under continued stirring. The reaction mixture was transferred into an oil bath at 35°C and was allowed to stand for 40 minutes. The beaker was returned to the ice bath, and 184 mL of water was added very slowly dropwise through the use of a separatory funnel. The beaker was again transferred to the oil bath, whose temperature was now set to 95°C. After 15 minutes, the beaker was returned to the ice bath, after which 400 mL of water was added dropwise. Thereafter, hydrogen peroxide (30%) was added slowly, which caused the changing of the color of the solution from dark brown to yellow as well as the formation of bubbles, until such time that no more bubbles were formed. The solution was centrifugated at 4000 rpm for 10 minutes, after which the liquid portion was drawn off. In order to remove the metal ions, the residue, containing the graphite oxide, was washed with hydrochloric acid for three times by addition of 5% HCl and centrifugation for 4000 rpm for 10 minutes. Washing with water was performed afterwards, with the same procedure as that of HCl, except that water was added and centrifugation was done for 30 minutes. After each stage, the liquid upper portion was discarded. This was also done three times. After washing with water, the solution was sonicated for 5 hours to ensure the complete exfoliation of graphite oxide into graphene oxide. The solution was again centrifugated for 30 minutes at 10000 rpm. This time, the upper liquid portion from each tube was collected and is called the "supernatant" while the residue was discarded. Each batch produced approximately one liter of supernatant, which was a GO suspension in water.

2.2.2. Synthesis of Hybrid Composite Aerogel. This suspension was then mixed with the bio-based polymer, which was chosen to be alginic acid (AA). The hydrogel was synthesized by a sol-gel method similar to that of Rassis et al. [14] but modified to incorporate the addition of GO as in the method of Alhwaige et al. [12].

An amount of supernatant was obtained and diluted with enough water to make a 25-mL solution of desired concentration of GO. Alginic acid weighing 0.625 g was added and left under constant stirring for at least 7 hours. Sodium hexametaphosphate (0.375 g) was added and stirred for half an hour, followed by the addition of calcium hydrogenphosphate dihydrate (0.474 g) and was mixed for another hour at 40°C. Lastly, GDL weighing 0.375 g was added and stirred for five minutes at room temperature. The solution was transferred into moulds and stored at 4°C for at least 15 hours for gelation.

The hydrogels were subjected to a four-step solvent exchange from water to ethanol, using a series of increasingly concentrated mixtures of ethanol and water: 50% (v/v) for 2 hours, 75% for 2 hours, 100% for 12 hours, and another 100% for 24 hours to ensure the complete exchange of solvent from water to ethanol.

The hydrogels were then converted into aerogels using supercritical drying using scCO₂. The solvent exchange was necessary because water is not miscible in liquid CO₂. The gels, now containing ethanol, are submerged in liquid CO₂ for 12 hours to replace the ethanol with CO₂. Afterwards, the pressure was increased to 10 MPa and the temperature to 40°C to turn the CO₂ into its supercritical state. The pressure was then released very slowly until atmospheric, and the aerogels were retrieved.

2.2.3. Characterization Techniques. The HCAs were then subjected to several characterization techniques, such as scanning electron microscopy (SEM), X-ray diffraction (XRD), thermogravimetric analysis (TGA), nitrogen adsorption-desorption measurements (also known as BET method), and Fourier Transform Infrared Spectroscopy (FTIR). SEM images were taken using JEOL JSM-7600F Field Emission Scanning Electron Microscope with an acceleration voltage of 3.0 kV. XRD was conducted using Rigaku MiniFlex with a voltage of 40 kV and a current of 15 mA using Cu-K α as source. The thermogravimetric analyzer used was Seiko TG/DTA 6300 operating from 35°C to 550°C with a ramp rate of 10 C°/min and aluminum pan as holder of the sample. For the BET measurements, BELSORP-mini II was used. The samples were first dried by heating to 90°C for 6 hours under high vacuum to drive off all the excess moisture and other adsorbed material. The measurements were then conducted at -196°C using nitrogen gas. The FTIR spectra of the samples were obtained using JASCO FT/IR-4100. The sample was crushed with anhydrous KBr in a ratio of roughly 1:9. The mixture was made into a pellet before insertion into the machine.

3. Results and Discussion

3.1. Characterization of the Graphene Oxide

The XRD pattern of graphene oxide is shown in Figure 1. A characteristic peak was observed at around

10°, which is consistent with that reported in numerous studies found in literature. The weak and broad peak at 21° is due to the glass holder that was used in the characterization and is present in all diffraction patterns in this study.

The FTIR spectrum of the graphene oxide is shown in Figure 2. The wide band found in the 3700-3000 cm⁻¹ range indicates the presence of hydroxyl groups, while the several small peaks on the right of 2000 cm⁻¹ are indicative of other oxygen-containing groups, such as carbonyl and epoxides. The weaker intensity possessed by the latter groups as compared to the hydroxyl band suggests the relative abundance of the hydroxyl groups, which is indeed the case in graphene oxide.

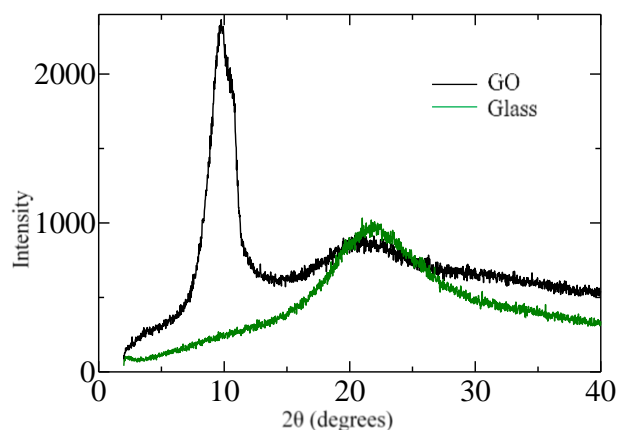


Figure 1. XRD Pattern of Graphene Oxide

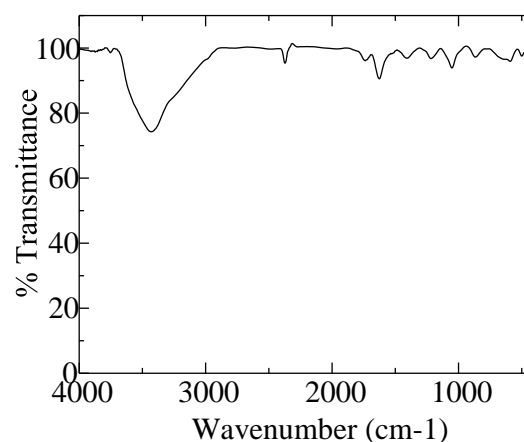


Figure 2. FTIR Spectrum of Graphene Oxide

3.2. Characterization of the Hybrid Composite Aerogel

The supernatant of graphene oxide whose properties have been discussed in the previous section was mixed with alginic acid (AA) in different proportions and made into aerogels. The aerogels were very light, as expected of an aerogel, has a visibly porous structure, and was relatively brittle. Figure 3 shows the aerogels produced with different concentrations of graphene oxide. On average, each monolith is 15.2 mm in diameter and 14.7 mm in height. They have masses ranging from 0.25-0.30 grams, and rough calculations provide a density of 0.10-0.15 g/cm³. Qualitatively, it can be observed that the color of the monoliths became darker with increasing GO concentration.

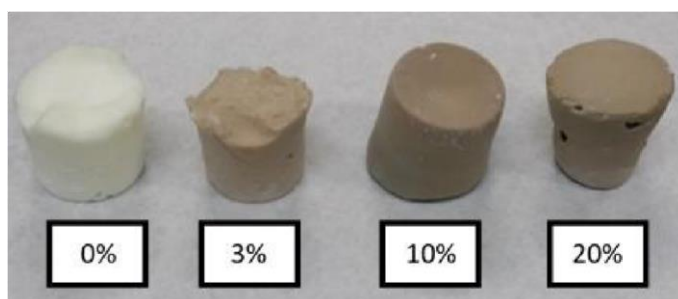


Figure 3. Hybrid Composite Aerogels with varying GO concentration

In order to determine the functional groups present in the hybrid composite aerogel, Fourier Transform Infrared Spectroscopy (FTIR) was performed. The FTIR spectra of aerogels with different GO concentrations are as shown in Figure 4. The graphs show a progression, with the peaks generally becoming more intense with increasing GO concentration.

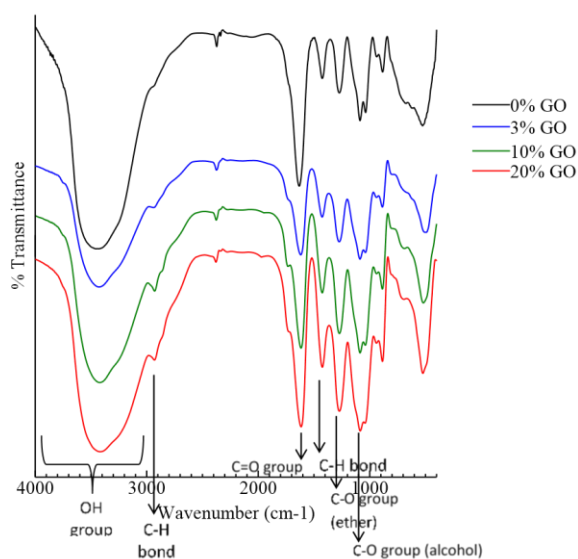


Figure 4. FTIR Spectra of HCAs with Various GO concentrations

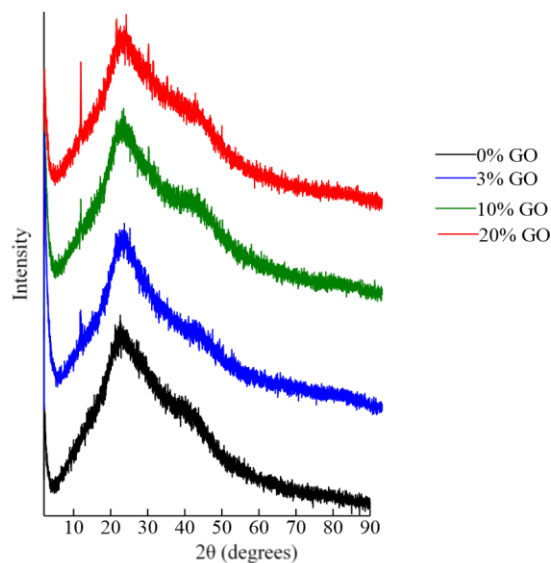


Figure 5. XRD Patterns of HCAs with Various GO concentrations

The FTIR spectra show consistent peaks across all concentrations of graphene oxide. Many of the peaks are attributable to the functionalities present in alginic acid and graphene oxide, such as the hydroxyl group, carbonyl group, and ethers.

The presence of graphene oxide in the aerogel was verified using X-ray diffraction (XRD). The diffraction patterns of the aerogels containing different GO concentrations are shown in Figure 5. The patterns are consistent, with peaks at 2° and 24° and a soft peak at around 42° . A very sharp peak at 11° is not present in pure alginic acid aerogel, yet is present in samples containing graphene oxide. This peak is characteristic to that of graphene oxide, as is shown in Figure 1 and is an indication that it is indeed contained in the aerogel. As the concentration of graphene oxide is increased from 0% to 20%, it can be observed that the peak at 11° also increases in intensity, which is supportive to the claim that the GO is incorporated in the aerogel.

The thermal stability of the aerogels is important because it determines the range of applications it can be intended for. In order to determine the thermal stability, thermogravimetric analysis (TGA) was performed on the samples. The temperature range tested was from 35°C to 550°C . The TGA curves show the percentage of the original mass remaining upon reaching a certain temperature, while the differential thermogravimetric curve (DTG) plots the intensity of the change in the mass of the sample with respect to the temperature. The TGA curves of the different samples are shown in Figure 6. In addition, the TGA and DTG curves of pure GO is added for comparison. The curves across all aerogel samples are similar, ending at roughly 50% of the original weight after reaching 550°C . Furthermore, there is no observable trend in the remaining weight of the sample at a particular temperature with respect to the concentration of GO.

The differential thermogravimetric curve shows the fastest decrease in mass occurring at $50\text{--}60^\circ\text{C}$ and from $200\text{--}300^\circ\text{C}$. The same curve for GO show peaks at $150\text{--}200^\circ\text{C}$ and $350\text{--}400^\circ\text{C}$. This suggests that GO did not increase the thermal stability of the aerogel, nor does it significantly affect the thermal performance of the aerogel at any specified temperature within the range tested. From this information, it can be inferred that the hybrid composite aerogel cannot be used at temperatures higher than 150°C .

The curves obtained are consistent with the findings of Soares et al. [15]. The first peak corresponds to the dehydration of alginic acid, while the second peak corresponds to its decomposition. Dehydration reaction occurs between carboxylic acid groups, forming an acid anhydride. The residue obtained after the decomposition process was a carbonaceous material, which is also consistent with the results obtained, which was a black powdery substance. In theory, the black

carbonaceous residue is largely composed of the carbon backbone of the aerogel. Due to the heating, the functional groups present in the calcium alginate structure have broken off, and a residue containing mostly carbon remains, thereby accounting for its black color.

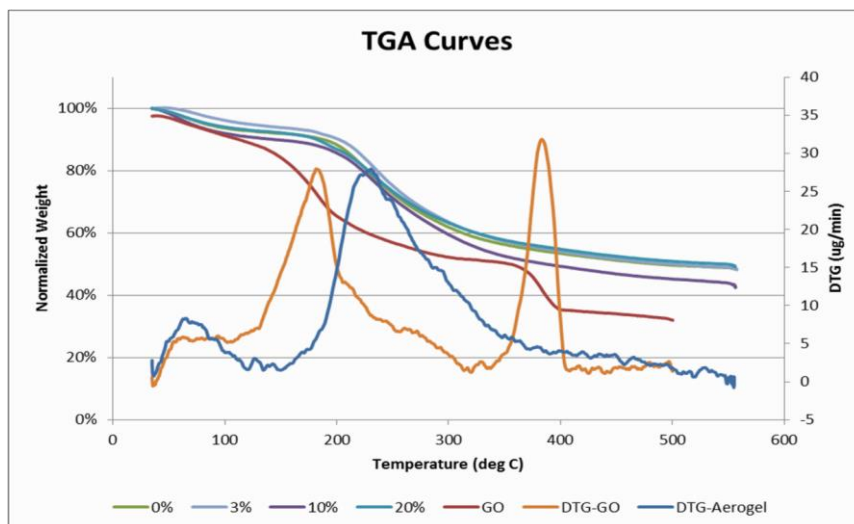


Figure 6. TGA Curves of pure GO and HCAs with various GO concentrations

From the SEM images as shown in Figure 7, all of the samples were observed to exhibit mesoporous and macroporous cavities, which strongly suggest the successful creation of an aerogel. The increase in GO concentration appears to create a more spongy morphology (Fig. 7.c and 7.d), as opposed to the rather dense appearance of the GO-free sample (Fig. 7.a). GO is known to act as a nanofiller, which probably assisted in the uniformity and mesoporosity of the material as it was synthesized during the sol-gel process. This can also explain the increase in the BET surface area as GO is introduced in the alginic acid aerogel, which is discussed further below.

The results from the nitrogen adsorption-desorption measurements are summarized in Table 1. It shows that addition of graphene oxide, in general, increases V_m , the monolayer nitrogen volume adsorbed on the surface of the material, the surface area and the pore volume. The highest values of these characteristics were observed at 10% concentration of graphene oxide. The observed lowering of these characteristics when the concentration was further increased to 20% may be explained by graphene oxide being too concentrated inside the aerogel, thereby being “crowded” and reducing the effective surface area and pore volume of the hybrid composite aerogel. Too small pore diameters pose difficulty for adsorbates to enter into pores and be adsorbed, whereas too large diameters cause the lowering of selectivity and general activity of the material, thus, mesopores, characterized by pore diameters ranging from 2-50 nm, are ideal for this application. The synthesized aerogels are in close range with this and are satisfactory.

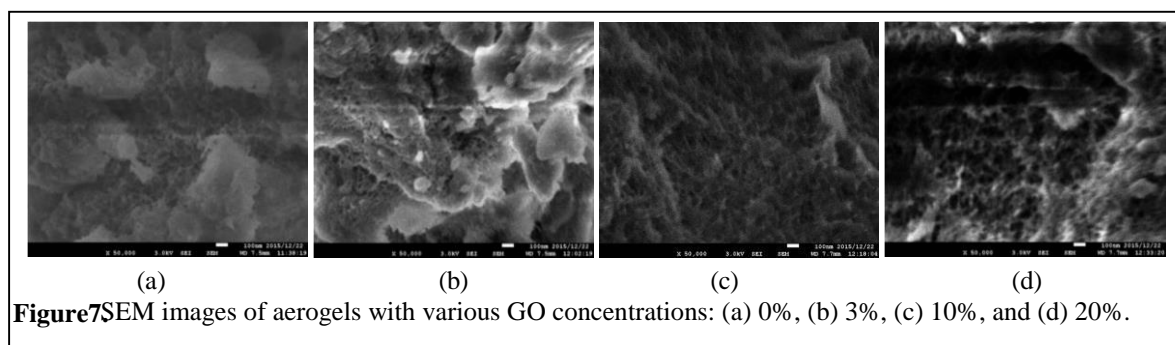


Figure 7 SEM images of aerogels with various GO concentrations: (a) 0%, (b) 3%, (c) 10%, and (d) 20%.

Table 1. Data from Nitrogen Adsorption-Desorption Measurements

Sample	V _m ³ (cm ³ STP/g)	S Area ² (m ² /g)	Pore Volume ³ (cm ³ /g)	Average Pore Diameter (nm)	Apparent Porosity
0% GO	23.250	101.19	1.3695	54.133	0.9250
3%	29.657	129.08	1.2814	39.707	0.9292
10%	40.726	177.26	2.9584	53.219	0.9268
20%	32.871	149.07	1.5561	43.505	0.9081

4. Conclusions

Hybrid composite aerogels composed of alginic acid and graphene oxide of various concentrations were successfully synthesized. Findings from analyses using FTIR, XRD, BET and SEM support the successful incorporation of graphene oxide in the alginic acid aerogel. This aerogel can be used as an adsorbent because of its porosity, and is a promising material for various applications.

References

- [1] Sitko R, Turek E, Zawisza B, Malicka E, Talik E, Heimann J Wrzalik R 2013 Adsorption of divalent metal ions from aqueous solutions using graphene oxide. *Dalton Trans.* **42** 5682-5689
- [2] Sun L, Yu H, & Fugetsu B 2012 Graphene oxide adsorption enhanced by in situ reduction with sodium hydrosulfite to remove acridine orange from aqueous solution. *J. Hazard. Mat.* **203** 101-110
- [3] Li Y, Du Q, Liu T, Sun J, Wang Y, Wu S Xia L 2013 Methylene blue adsorption on graphene oxide/calcium alginate composites. *Carbohydrate Poly.* **95** 501-507
- [4] Kizzie A, Wong-Foy A, & Matzger A 2011. Effect of humidity on the performance of microporous coordination polymers as adsorbents for CO₂ capture. *Langmuir* **27** 6368-6373.
- [5] Yu K, Kiesling K, & Schmidt J 2012 Trace Flue Gas Contaminants Poison Coordinatively Unsaturated Metal–Organic Frameworks: Implications for CO₂ Adsorption and Separation. *J. Phy. Che. C* **116**(38) 20480-20488.
- [6] Garcia-Gonzalez C, Alnaief M, & Smirnova I 2011 Polysaccharide-based aerogels – Promising biodegradable carriers for drug delivery systems. *Carbohydrate Poly.* **86** 1425-1438.
- [7] Mehling T, Smirnova I, Guenther U, & Neubert R 2009 Polysaccharide-based aerogels as drug carriers. *J. of Non-Crystalline Solids* **355** 2472-2479.
- [8] Gupta V K, Carrott P, Ribeiro Carrott M M L, and Suhas 2009 Low-Cost Adsorbents: Growing Approach to Wastewater Treatment—a Review. *Critical Rev. in Environ. Sci.* **35**(5) 783-842
- [9] Yu C H, Huang C H, & Tan C S 2012 A Review of CO₂ Capture by Absorption and Adsorption. *Aerosol and Air Quality Res.* **12** 745-769. doi:10.4209/aaqr.2012.05.0132
- [10] Biedermann A (n.d.). *Aerogel Drying*. Retrieved April 4, 2015, from Introduction to Aerogels and Sol-Gel Science: <http://people.virginia.edu/~amb4ht/aeroDrying.html>
- [11] Husing N, & Hartmann S 2009. Inorganic–Organic Hybrid Porous Materials. In L. Merhari, *Hybrid Nanocomposites for Nanotechno.: Elect., Opt., Magnetic and Biomed. App.* (pp. 131-172). New York: Springer Science+Business Media.

- [12] Alhwaige A A, Agag T, Ishida H, & Qutubuddin S 2013. Biobased chitosan hybrid aerogels with superior adsorption: Role of graphene oxide in CO₂ capture. *RSC Adv.* **31** 6011-16020.
- [13] Koinuma M, Ogata C, Kamei Y, Hatakeyama K, Tateishi H, Watanabe Y, Matsumoto Y. 2012. Photochemical engineering of graphene oxide nanosheets. *The J. Phy. Che. C* **116** 19822-19827.
- [14] Rassis D, Nussinovitch A, Saguy I S 1997 Tailor-made porous solid foods. *Int. J. Food Sci. Techno.* **32**(4) 271–278
- [15] Soares J P, Santos J E, Chierice G O, & Cavalheiro E T 2004 Thermal behavior of alginic acid and its sodium salt. *Eclética Química* **29**(2) 53-56